Engineered Osmosis for Energy Efficient Separations: Optimizing Waste Heat Utilization

DOE Award Number: DE-EE0003467

Project Period: 08/16/2010 – 10/15/2012
Final Report Issued: 01/13/2013

Principal Investigator:
Nathan T Hancock, PhD
617-599-8253
21 Drydock Avenue
Suite 21-730
Boston, MA 02210

Recipient Organization:
Oasys Water Inc.
21 Drydock Avenue
Suite 21-730
Boston, MA 02210

Executive Summary

The purpose of this study is to design (i) a stripper system where heat is used to strip ammonia (NH_3) and carbon dioxide (CO_2) from a diluted draw solution; and (ii) a condensation or absorption system where the stripped NH_3 and CO_2 are captured in condensed water to form a re-concentrated draw solution.

This study supports the Industrial Technologies Program of the DOE Office of Energy Efficiency and Renewable Energy and their Industrial Energy Efficiency Grand Challenge award solicitation. The study is divided into five primary tasks:

- *Task 1*: Assessment of potential benefits associated with integrated Oasys engineered osmosis (EO™) technology into existing water treatment schemes.
- *Task 2*: Selection of operating conditions for pilot design and testing using industrial waste heat.
- *Task 3*: Development of a stripper subsystem capable of removing thermolytic solutes to produce high quality product water within the EO system framework.
- *Task 4*: Development of a condensation or absorption subsystem capable of recapturing draw solution vapor for reuse as draw solution within the EO system framework.
- *Task 5*: Modeling the striper and condenser/absorption system performance using process simulation programs with modified property libraries suitable for Oasys draw solution chemistries.

Results from this study show that simulated Oasys draw solutions composed of a complex electrolyte solution associated with the dissolution of NH_3 and CO_2 gas in water can successfully be stripped and fully condensed under standard atmospheric pressure. Stripper bottoms NH_3 concentration can reliably be reduced to < 1 mg/L, even when starting with liquids that have an NH_3 mass fraction exceeding 6 % to simulate diluted draw solution from the forward osmosis membrane component of the process. Concentrated draw solution produced by fully condensing the stripper tops was shown to exceed 6 M-C with nitrogen-to-carbon (N:C) molar ratios on the order of two. Reducing the operating pressure of the stripper column serves to reduce the partial vapor pressure of both NH_3 and CO_2 in

solution and enables lower temperature operation towards integration of industrial low-grade or waste heat. Effective stripping of solutes was observed with operating pressures as low as 100 mbar (3-inHg). Systems operating at reduced pressure and temperature require additional design considerations to fully condense and absorb these constituents for reuse within the Oasys EO system context.

Comparing empirical data with process simulation models confirmed that several key parameters related to vapor-liquid equilibrium and intrinsic material properties were not accurate. Additional experiments and refinement of material property databases within the chosen process simulation software was required to improve the reliability of process simulations for engineering design support. Data from experiments was also employed to calculate critical mass transfer and system design parameters (such as the height equivalent to a theoretical plate (HETP)) to aid in process design. When measured in a less than optimal design state for the stripping of NH_3 and CO_2 from a simulated dilute draw solution the HETP for one type of commercial stripper packing material was 1.88 ft/stage.

During this study it was observed that the heat duty required to vaporize the draw solution solutes is substantially affected by the amount of water boilup also produced to achieve a low NH_3 stripper bottoms concentration specification. Additionally, fluid loading of the stripper packing media is a critical performance parameter that affects all facets of optimum stripper column performance. Condensation of the draw solution tops vapor requires additional process considerations if being conducted in sub-atmospheric conditions and low temperature.

Future work will focus on the commercialization of the Oasys EO technology platform for numerous applications in water and wastewater treatment as well as harvesting low enthalpy energy with our proprietary osmotic heat engine. Engineering design related to thermal integration of Oasys EO technology for both low and high-grade heat applications is underway. Novel thermal recovery processes are also being investigated in addition to the conventional approaches described in this report. Oasys Water plans to deploy commercial scale systems into the energy and zero liquid discharge markets in 2013. Additional process refinement will lead to integration of low enthalpy renewable heat sources for municipal desalination applications.

Acknowledgment: This report is based upon work supported by the U. S. Department of Energy under Award No DE-EE0003467.

Disclaimer: Any findings, opinions, and conclusions or recommendations expressed in this report are those of the author(s) and do not necessarily reflect the views of the Department of Energy.

Table of Contents

Executive Summary ... ii

Table of Contents ... v

List of Figures ... vi

List of Tables ... vii

Introduction ... 2

Background ... 4

- **Project objectives** ... 6

Material and Methods ... 7

- **Stripper systems** ... 7
- **Absorption systems** ... 10

Results and Discussion ... 13

- **Task 1: Potential Benefits Assessment** ... 13
- **Task 2: Selection of Operation Conditions for Testing Using Industrial Waste Heat** ... 15
- **Task 3: Stripper Subsystem Development** ... 19
- **Task 4: Absorption Subsystem Development** ... 21
- **Task 5: Modeling the Absorption and Stripper Columns Performance** ... 23
- **Accomplishments** ... 27

Conclusions ... 28

Recommendations ... 29

References ... 30

List of Figures

Figure 1: Diagram of the Oasys Water EO™ platform for desalination. 3

Figure 2: Oasys technology comparison to conventional desalination technologies. 6

Figure 3: Schematic diagram of SRI stripper system. 9

Figure 4: Photographs of pilot stripper and absorber system and screen capture of associated human machine interface of the data acquisition and control system. 10

Figure 5: Schematic diagram of the bench-scale absorber. 11

Figure 6: Schematic diagram of knockout pot batch absorption system. 12

Figure 7: Photograph of knockout pot batch absorption system. 12

Figure 8: The effect of pressure on CO_2 absorption rate at 21 ˚C. 16

Figure 9: The effect of liquid recirculation rate at 22˚ C and 180 mbar. 17

Figure 10: Percent removal of NH_3 calculated by measurements of NH_3 in the bleed solution as a function of temperature, pressure, and feed flow rate. 18

Figure 11: Residual level of ammonia in the stripper bottoms water as a function of the number of throughput cycles (correct for small changes in the feed concentration at various stages). 19

Figure 12: Vapor rate as a function of reboiler duty for tests conducted at atmospheric pressure. 20

Figure 13: Reactor tops temperature as a function of time for a representative absorption experiment. 22

Figure 14: Parity plot of the measured and process simulation calculated total pressure for a variety of NH_3/CO_2 mixtures. 24

Figure 15: Parity plot of the measured and process simulation calculated partial pressure of CO_2 for a variety of NH_3/CO_2 mixtures. 25

Figure 16: Parity plot of the measured and process simulation calculated solution density for a variety of NH_3/CO_2 aqueous mixtures. 25

List of Tables

Table 1: Summary of testing conditions during various runs with advanced pilot scale stripper column. Concentrated draw solution (CDS) produced by stripping the NH_3 and CO_2 from the solution and fully condensing the vapor. 21

Table 2: Experiment parameters and associated mass and energy balance to determine the extent of $CO_2NH_2^-$ conversion.. 23

Table 3: Comparison of stripper process experimental run with simulated process results and subsequent key process performance parameters... 26

Introduction

Osmotically driven membrane processes (ODMPs) are an emerging class of water treatment and renewable energy production technologies that employ osmotic pressure gradients to perform useful separations [1-3]. For water treatment, ODMPs employs an engineered draw solution with a higher osmotic pressure than the feed stream to extract water from the feed through a semi-permeable membrane [4]. These processes are proven to be technically viable for treatment of highly impaired feed water supplies through a number of process configurations including direct osmotic concentration or dilution [5-10] and forward osmosis (FO) [11-13].

The FO process is the focus of the work presented here. Recent research performed at the bench- and low capacity pilot-scale has demonstrated the robust nature of FO processes to treat highly impaired water streams with minimal pretreatment compared to established pressure or thermally driven processes for desalination [14-17]. However, traditional implementation of FO systems incorporates energy intensive methods to reconcentrate the draw solution and often relies upon reverse osmosis (RO) to perform the work. Hybrid FO-RO systems are demonstrated to produce high quality product water from a variety of feed streams with relatively low salinity (e.g., between 500 and 5,000 mg/L) [8, 18-20]. However, if the RO subsystem is the primary means for reconcentrating the draw solution, it both limits the salinity that may be treated due to osmotic pressure limitations of the RO subsystem and is not energetically favorable [20, 21].

To improve the viability of FO processes for desalination it is preferable to employ alternative means to reconcentrate the draw solution. One alternative method identifies the use of a thermolytic solution consisting of dissolved ammonia and carbon dioxide salts [22, 23]. In this process, a draw solution consisting of a mixture of NH_4HCO_3 and $NH_4CO_2NH_2$ with a nitrogen-to-carbon (N:C) molar ratio in excess of one is employed to extract water from a feed stream. As water is extracted from the feed stream it dilutes the draw solution. The diluted draw solution is then heated, which forces the thermolytic salts to decompose into ammonia and carbon dioxide gas. These gases may then be captured and condensed or absorbed to form a concentrated draw solution. Oasys Water Inc. was founded in 2008 to commercialize these types of thermolytic solutions for a variety of desalination applications. A diagram of the Oasys Water engineered osmosis (EO™) system is shown in Figure 1.

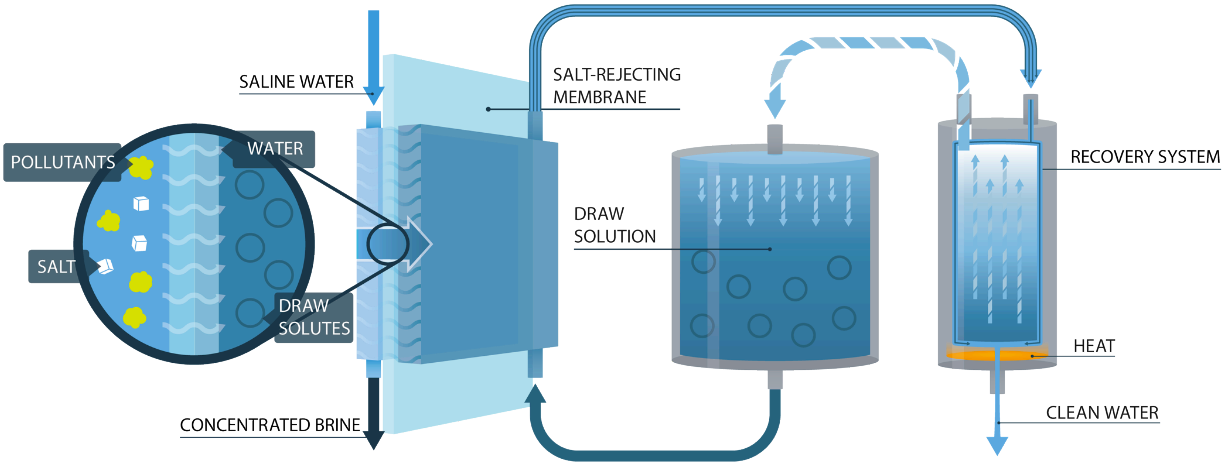

Figure 1: Diagram of the Oasys Water EO™ platform for desalination.

This process has several potential advantages over conventional methods of desalination. Employing draw solutions with osmotic pressures significantly exceeding ~700 psi (the approximate limit for standard electrolyte based draw solutions in FO-RO hybrid systems) expands the operating envelope of the process to enable treatment of highly saline brines. Our recent publication [24] evaluated the specific energy required to produce 1 kg of water from a feed stream of 70,000 mg/L TDS, while concentrating the stream to 200,000 mg/L TDS, with conventional thermal evaporation versus the Oasys EO method. This work identified the theoretical minimum specific energy required to produce 1 kg of product water in the case of a single stage evaporator is 633 W-h/kg. To produce the same amount of water with an NH_3/CO_2 FO system, 102 W-h/kg would be required. These calculations demonstrate that for a concentrated saline feed, under ideal conditions, it requires approximately two times more energy, per kg of purified water produced, to purify the stream by evaporation of water rather than by evaporation of ammonia and carbon dioxide gases from an FO draw solution. Real engineered FO systems, although unlikely to fully achieve these theoretical energy requirements, do in practice derive their energetic advantage from this fundamental difference in required energy input.

Background

There are three primary classes of established technologies for desalination of water. These include pressure driven membrane, thermally driven evaporative, and electrically driven processes [25]. Electrically driven processes such as electrodialysis (ED), ED reversal (EDR), and capacitive deionization (CDI) are typically used to desalination low salinity streams or for ultra-pure water production. To desalinate brackish water and seawater the dominant membrane processes such as nanofiltration (NF) and reverse osmosis (RO) are typically employed. These technologies are favored over thermal evaporative processes for the desalination of moderate salinity feed streams due to the ability of the process to desalinate water by permeation through a semipermeable membrane rather than incur the enthalpic penalty of a phase vapor phase change [26]. Pressure driven membrane processes have also benefit significantly from the optimization and wide scale employment of pressure recovery devices to reuse pressure-volume work within the system, which has enabled these processes to operate near the thermodynamic minimum energy for separation of water from saline water (~1 kWh/m^3) [27].

Yet, pressure driven membrane processes are limited in their ability to treat high salinity brines because the osmotic pressure of these solutions would force the process to operate at prohibitively large hydraulic pressures in excess of the material constraints of these systems [28]. To treat high salinity brines it is often necessary to evaporate water either by contact with a heat exchange surface or by permeation through a hydrophobic membrane as in the case of membrane distillation (MD). MD systems are the focus of continued research, but to date there are no commercial installations of note for this process, and commercialization is generally hampered by suboptimal membrane materials and difficulties related to thermal management within these systems [21]. Conversely, thermal evaporative processes like multi-effect distillation (MED), multi-stage flash (MSF) evaporation, and vapor compression (VC) are widely used for desalination [29]. The enthalpy of vaporization for water is approximately 650 kWh/m^3 and is approximately the specific thermal energy required by a single stage evaporator to produce a cubic meter of water. Fortunately, there are a number of process modifications that can be made with respect to heat integration to substantially improve the efficiency of evaporators. The most common modification is to change the pressure regime within various evaporation stages of a system to allow for efficient reuse of the energy dissipated by the condensing water vapor. The efficiency measure commonly employed for MED and MSF systems is the gained output ratio (GOR), which is the ratio of the unit mass of water produced per unit mass of steam as energy invested. While these processes have inherently greater energy demand than pressure driven membrane processes, many installations are designed with GOR values between 5 and 15 to substantially reduce thermal energy demand of these systems compared to the case of a single stage evaporator [21].

FO systems that employ thermolytic solutes provide a compelling fit between thermally driven evaporative processes and pressure driven membrane processes by providing similar high salinity brine treatment capabilities as evaporators with many of the cost and operations benefits of membrane systems. The first iteration of the Oasys membrane brine concentrator (MBC) is shown with respect to conventional processes for desalination in Figure 2. A second Oasys technology that integrates with low enthalpy renewable thermal energy sources or cogeneration systems with available low-grade heat is also shown. Here the thermal energy required for the system may be recovered from systems that are not able to economically produce energy in their respective contexts.

The specific area being addressed in this study is the thermal recovery system of the Oasys EO platform for brine treatment. Here we seek to leverage existing process modelling software with the best available chemical kinetics and vapor-liquid equilibrium data to provide a powerful systems engineering tool for further optimization and evaluation of various heat integration designs employed for the Oasys system.

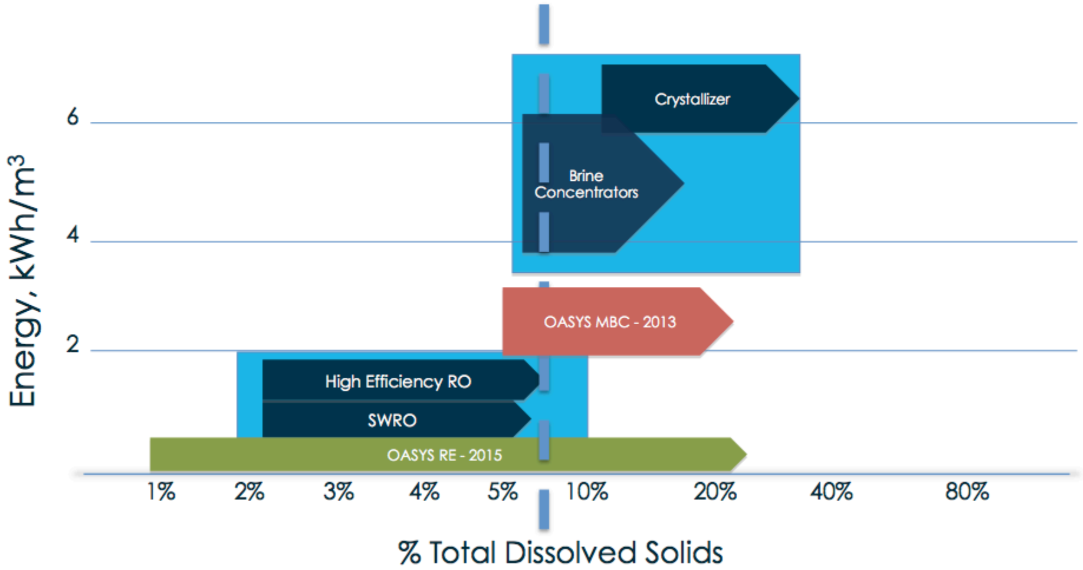

Figure 2: Oasys technology comparison to conventional desalination technologies.

Project objectives

The objectives of this project are (i) to improve the design of the stripper system to strip ammonia and carbon dioxide from a diluted draw solution, and (ii) to improve the design of a condensation or absorption system where the stripped ammonia and carbon dioxide are captured in condensed water to form a reconcentrated draw solution.

To accomplish these objectives vapor-liquid equilibrium data for various ammonia and carbon dioxide systems under different temperature and pressure regimes were collected from a variety of literature sources as well as experimentally. A process simulation software package (AspenPLUS, Aspen Tech Inc., Burlington, MA) was employed to incorporate this data into effective models for simulation of the Oasys stripping subsystem. Kinetics data was procured through empirical correlations that employed a custom vapor absorption apparatus to explore the speed and heat of reaction for the absorption of CO_2 gas into an aqueous ammonia solution. This data was integrated with the process simulation software and used to refine the engineering design of the absorption and condensation subsystem. To accomplish the study goals, the study is divided into five primary tasks:

1. Potential benefits assessment
2. Select operation conditions for pilot design and testing using industrial waste heat

3. Stripper subsystem development
4. Absorption subsystem development
5. Modeling of the stripper and absorption columns performance

Four Oasys employees with the aid of some contractors primarily conducted this work:

- Nathan Hancock, PhD (PI from 8/1/12 through completion): Accomplished Environmental Science and Engineering PhD (Colorado School of Mines) with extensive experience in the application of novel and established membrane processes for treatment of impaired water, aqueous chemistry, and physicochemical separation processes. Capabilities include leading strategic R&D priorities and staff, innovative process engineering for water treatment, and numerical modeling.
- Robert McGinnis, PhD (PI from 8/16/10 through 8/1/12): Founder of Oasys Water Inc. Performed pioneering work on NH_3/CO_2 based draw solution for FO at Yale University. Generated numerous publications and other technical releases on various aspects of this approach for desalination and energy production.
- Marek Nowosielksi, PE, C.Eng: led the Oasys design team and the demonstration of the company's first product – the Membrane Brine Concentrator (MBC). Prior to joining Oasys Water he was responsible for the design of membrane-based water treatment plants for GE Water and Process Technologies and plant optimization with DuPont. Marek earned his MEng in Chemical Engineering from the University of Cambridge, his M.Sc from Cranfield University and his MBA from Babson College.
- Ronald Ewan: Lead chemical operator with primary responsibility for test system fabrication and empirical data gathering.

Material and Methods

Stripper systems

For tasks two through four, three different experimental systems were used to evaluate the impact of various critical operating parameters on the overall efficiency of removing NH_3 and CO_2 from solutions. The first effort was performed in collaboration with the

Stanford Research Institute (SRI, Menlo Park, CA) and focused on stripping ammonia and carbon dioxide from a 2.8 M-N solution with 50 ˚C heat under sub-atmospheric pressure.

A bench-scale stripper system was constructed to determine the rate of rate of NH_3 and CO_2 removal from Oasys diluted draw solution (DDS). The system, shown schematically in Figure 3, consists of a 4-in diameter distillation column, reboiler, tanks, and circulating pump. The column height was varied from 8 to 16 ft. The reboiler was a stainless steel shell and tube heat exchanger heated by a hot fluid from an external electric heater. The system was operated under sub-atmospheric pressure using a high-capacity liquid-ring pump. A centrifugal pump at the bottom of the sump circulated the solution between the column sump and the reboiler. Steam from the reboiler was used as the stripping media. A metering pump injected the liquid at the top of the column and the liquid was preheated before it entered the stripper column. The solution now stripped of NH3 and CO2 was withdrawn from the reboiler circuit at a rate commensurate with the DDS feed rate to maintain a constant level in the sump. Pressure, temperatures, and liquid flow rates were recorded. The compositions of the feed solution and the bleed solution were determined by chemical analysis. The stripper packing had a surface area of 420 m^2/m^3 and a rated height equivalent to a theoretical plate (HETP) of 10-in/stage.

A second study was performed in collaboration with Artisan Industries Inc. (Waltham, MA) to demonstrate the coupled stripping and condensation/absorption process to recover the draw solution solutes at ambient pressure. The test setup consisted of a 4-in stripping column packed with 20 feet of stainless steel structured mesh packing, tankage, pumps, a shell-and-tube preheater, a U-tube condenser, and various temperature, pressure and flow metering instrumentation. Diluted draw solution was continuously metered to the stripping column by a feed pump controlled by a PID flow-control loop. A pre-heater and backpressure control valve were installed in the feed line to the stripper. After passing through the backpressure valve, the feed material typically flashed as it was exposed to the stripper operating pressure. A thermosiphon reboiler installed at the bottom of the stripping column was used to boil up water to provide the stream stripping media.

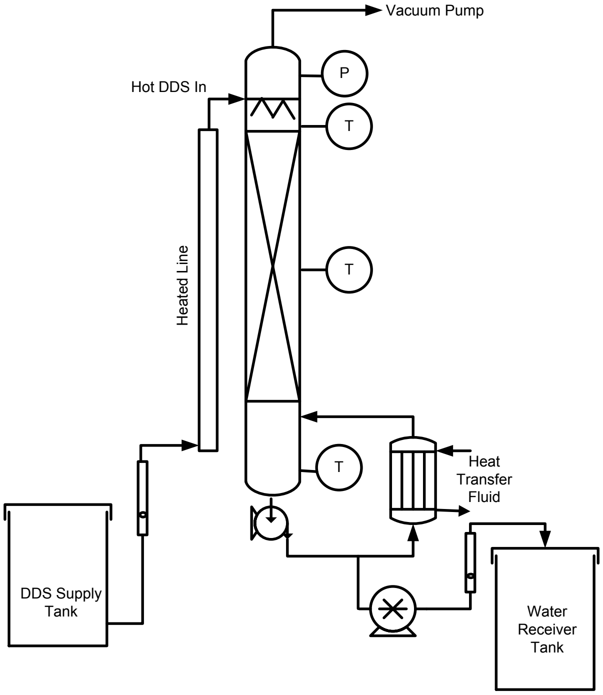

Figure 3: Schematic diagram of SRI stripper system.

The stripper bottoms effluent stream continuously drained into a receiver by gravity. The vapors exiting the top of the stripping column were condensed using a U-tube condenser cooled with a water/glycol mixture. It was possible to fully recover all of the stripper overheads as distillate in the condenser. All PID loops and data acquisition and monitoring of the process were controlled by a central data collection and programmable logic control system.

Additional experimental measurements to determine optimum operating parameters for stripper operations were obtained using a pilot scale system developed at the Oasys Thermal R&D facility (Somerset, MA). The pilot system shown in Figure 4 consists of 30 ft section of 4-in diameter stainless steel column filled with structured packing from the same vendor and make as anticipated for commercial installations. The experimental setup includes extensive instrumentation for temperature, pressure and flow measurements. The primary objective of the stripper testing includes the determination of reboiler heat duty for a given product purity from a given composition of the DDS.

Figure 4: Photographs of pilot stripper and absorber system and screen capture of associated human machine interface of the data acquisition and control system.

Absorption systems

Two absorption test systems were employed in this investigation. The first system was constructed in collaboration with SRI. A schematic diagram of the absorber system is shown in Figure 5. The absorber was a 5 in outside diameter stainless steel column, which contained a high surface area, mesh packing and was a total of 32-in tall. The packing had a surface area of 1900 m^2/m^3. An ammonium carbonate solution representative of DDS produced by the engineered osmosis process was circulated through the packing under sub-atmospheric pressure. CO_2 gas was introduced into the system to be absorbed by the solution and the rate of the gas injection was varied to maintain a constant pressure. A shell-in-tube heat exchanger was used to remove the heat generated by the absorption and maintain a constant temperature.

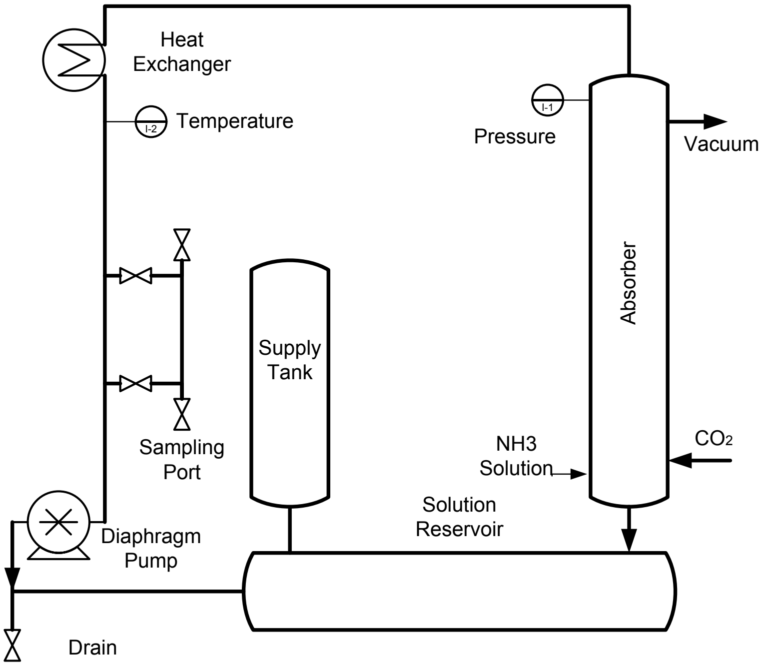

Figure 5: Schematic diagram of the bench-scale absorber.

A second system developed by Oasys Water was also used to derive additional kinetics data under atmospheric pressure conditions to aid in model development. In this system, CO_2 gas is bubbled into a mixture of aqueous NH_4OH and water through a sparging plate at the bottom of the knockout pot. The knockout pot is well insulated to capture the heat of reaction during the exothermic formation of CO2NH2-. The temperature increase of the solution is monitored as a function of time, and used to estimate the CO2NH2- formation reaction.

In addition to the empirical data sets derived through the use of the above-described systems, a comprehensive literature review was also conducted to identify pre-existing vapor-liquid equilibrium and kinetics data for ternary H_2O-NH_3-CO_2 systems. A review of over 30 publications on the topic rendered three studies that were of particular interest within the operating conditions of interest for this study. The first study was published by Göppert and Maurer in 1988 [30] focuses on vapor-liquid equilibria in aqueous solutions of NH_3 and CO_2 at temperatures between 333 and 393 K and pressures up to 7 MPa. The second study was published by Kurz et al. in 1995 [31] and focuses on the solubility of weak electrolyte gases including ternary H_2O-NH_3-CO_2 systems with a slightly larger temperature range between 310 and 470 K. The final publication of interest was published by Ghaemi et al. in 2009 [32] and focused on the absorption of CO_2 by carbonated ammonia solutions. Data from these studies was employed to refine the SYSOP15 and ElecNRTL thermophysical property databases of Aspen Plus.

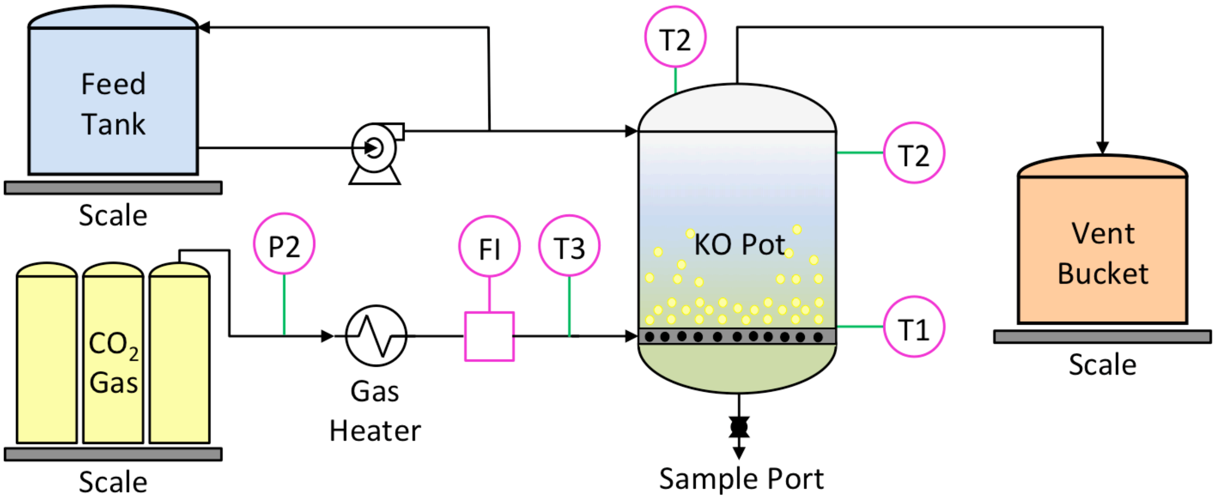

Figure 6: Schematic diagram of knockout pot batch absorption system.

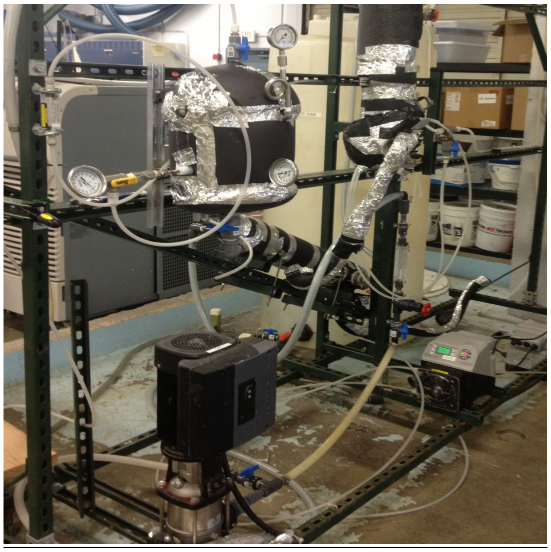

Figure 7: Photograph of knockout pot batch absorption system.

Results and Discussion

Task 1: Potential Benefits Assessment

For the purpose of this public disclosure only information disclosed in our recent publication [24] will be employed for the potential benefits assessment. Systems currently under development include several additional modifications to the heat integration scheme and overall process technology that will have significant impact on the energy consumption of the system. For MVC based EO™ systems with a combined heat and power system, consisting of an integrated natural gas engine and exhaust heat recovery unit, the estimated specific energy demand is approximately 21.3 kWh/m^3 of brine treated. For comparison, the best available forced circulation MVC employed for brine treatment with comparable capacity has a specific energy demand of approximately 34 kWh/m^3. To perform comparable treatment and achieve approximately 65% recovery from 70,000 mg/L TDS feed water, the Oasys EO system will require approximately 40% less energy. The potential domestic addressable market for this technology includes an estimated 38 million m^3 of high salinity produced water resulting from the extraction of unconventional hydrocarbon reserves each year and growing [33]. These systems are ready to commercialize presently, and it is feasible that by 2020 an estimated 19 million m^3 per year of produced brine could be treated by Oasys systems in this market. The total projected energy savings associated performing this treatment rather than using the next best available technology is approximately 820 Tbtu in 2020.

The economic benefits associated with this scenario are difficult to quantify because of the volatility of the natural gas market and substantial potential impact of government regulations on the need for producers to treat or dispose of produced waters generally. However, the cost of trucking produced water for disposal through Class I or II injection wells is known to cost between $20 and $160 per m^3 ($3 and $25 per bbl) and depends on several factors including hauling distance and the number of permitted injection wells in a region. On average the cost to treat this water with the Oasys process is below the cost of disposal. Additionally, numerous public stakeholders continue to voice concern over various environmental and health impacts associated with unconventional hydrocarbon recovery and management of toxic flowback and produced water in particular. Some of the public outcry has led to a reduction in the ability to permit new injection facilities and has also been speculated to substantially reduce the likelihood of fully developing domestic unconventional gas plays. Treatment systems that manage this wastewater resource appropriately may play a substantial role in improving public perception and increase the development potential of many water scarce plays.

It is best to use a specific case study to understand the environmental benefits of the Oasys technology. In the Marcellus shale of Pennsylvania alone there was estimated 3.4 trillion ft^3 (TCF) of proven shale gas reserves in 2009 [33]. It is estimated that approximately 200 gallons of produced water are generated for every million ft^3 (MMCF) of gas extracted from the Marcellus, which is relatively low compared to other basins such as the Barnett, Eagle Ford, or Haynesville that can be more than 2,000 gallons per MMCF. This does not include the substantial volume of fracture flowback water generated within these plays. An analysis of the potential environmental benefits of deploying Oasys technology for the treatment of produced water in the Marcellus shale is provided below. For this analysis the following assumptions are used:

- A 4,000 gallon truck averaging 10 miles per gallon of diesel fuel must drive an average of 100 miles to an injection facility and back
- The same truck would need to drive 20 miles and back to travel to a near field Oasys produced water treatment facility
- 75% of the proven shale gas reserves are produced by the year 2020, resulting in a total produced water volume of 510,000,000 gallons
- 122 lb of CO_2 are produced during the combustion of one standard MCF of natural gas
- 1.03 MMBTU per MCF of natural gas
- 22.4 lb of CO_2 are produced during the combustion of one gallon of diesel fuel
- The purified product water generated by the Oasys system may be discharged to a nearby surface water body
- The high-density brine generated by the process may be trucked back to the producer for reuse as a drilling fluid, completion fluid, or for other production activities.

Based on these assumptions it is trivial to calculate the total mass of CO_2 emissions reduced by using the Oasys process. In the case of trucking the produced water for disposal approximately 5,707 billion pounds (Glb) of CO_2 will be released to the atmosphere during the development of 75% of the 2009 proven reserves in the Marcellus. In the second case where the water is trucked to a near field treatment facility and treated with the Oasys process approximately 1,180 Glb of CO_2 will be released to the atmosphere with the Oasys treatment process accounting for only 370 Glb of CO_2. Deploying Oasys brine treatment technology rather than maintaining the status quo approach of trucking and injecting has the potential to reducing approximately 80% of the CO_2 emissions resulting from the development of domestic unconventional gas reserves in the Marcellus shale. This substantial relative reduction in CO_2 will be even greater in most other domestic unconventional gas plays where the ratio of the volume of produced water to natural gas extracted is even greater.

It is important to note that the energy savings and environmental benefits described in this section are limited to one potential application of Oasys EO technology. Additional development is underway to expand the operating envelope for the technology and enable such things as low enthalpy geothermal or solar thermal sources that cannot otherwise be used for electricity generation, but may be integrated with our technology to perform desalination of any stream up to approximately 250,000 mg/L TDS as seen in Figure 2.

Task 2: Selection of Operation Conditions for Testing Using Industrial Waste Heat

Absorber Analysis

The rate of CO_2 absorption as a function of the molar ratio of nitrogen to carbon (N:C rato) in the liquid at a temperature of 21° ±1°C is shown in Figure 8. At a solution recycle rate of 1 L/min (lpm), the rate of absorption increases with absorber pressure and N:C ratio of the solution. At low N:C ratios, the effect of pressure on the absorption is reduced, indicating that the N:C ratio is an important parameter with respect to the rate of CO_2 absorption. Although the data appears to be linear with respect to the N:C ratio, the absorption rate tends to increase with higher ratios within the mass transfer limit; this characteristic is evident on the data for the run at 280 mbar.

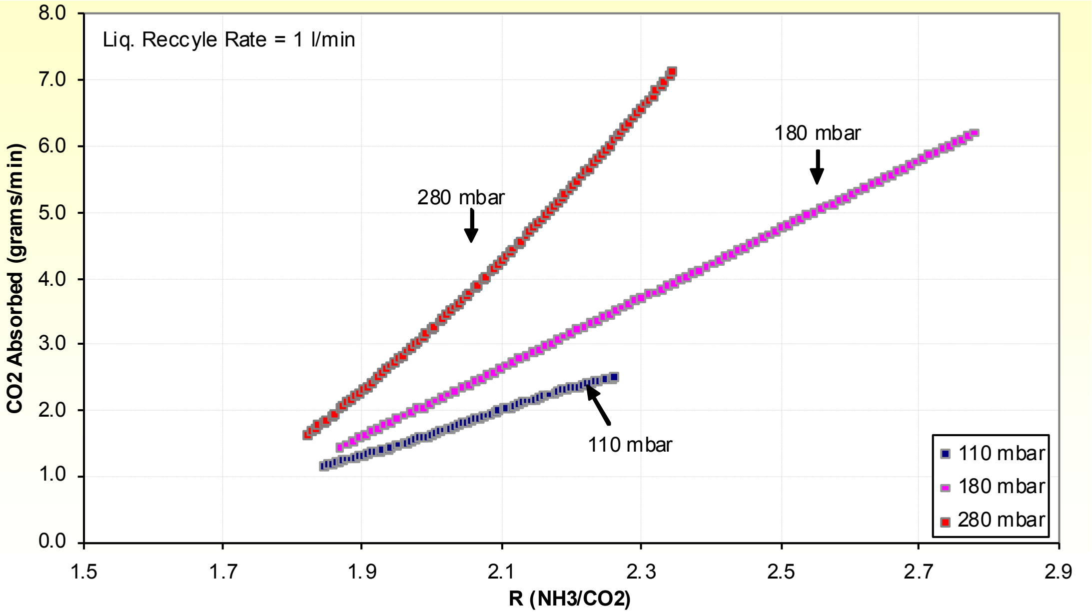

Figure 8: The effect of pressure on CO_2 absorption rate at 21 ˚C.

The solution recycling rate was also found to have an influence on the rate of CO_2 absorption as shown in Figure 9. As the liquid recycling rate increases from 1 to 2.2 lpm, the rate of absorption increases indicating that the packing is more wetted by the liquid at the higher flow rate than at the lower flow rate. However, increasing the recycling rate from 2.2 to 3.2 lpm did not appear to increase the absorption rate. The rate of CO2 absorption at a recycling rate above ~2.5 lpm can be used for the design of the absorber using this packing.

The absorption rate appears to reach a limiting value at a relatively low liquid recycle flow rate of ~3 lpm. Yet, a high surface area packing, especially in vacuum service, liquid flow rates exceeding those required to wet the surface of the packing can lead to high pressure drop. In vacuum distillation of hydrocarbons, a liquid flow rate of 10 m^3/m^2-h is typical and such a flow rate corresponds to 2 lpm for this bench-scale absorber.

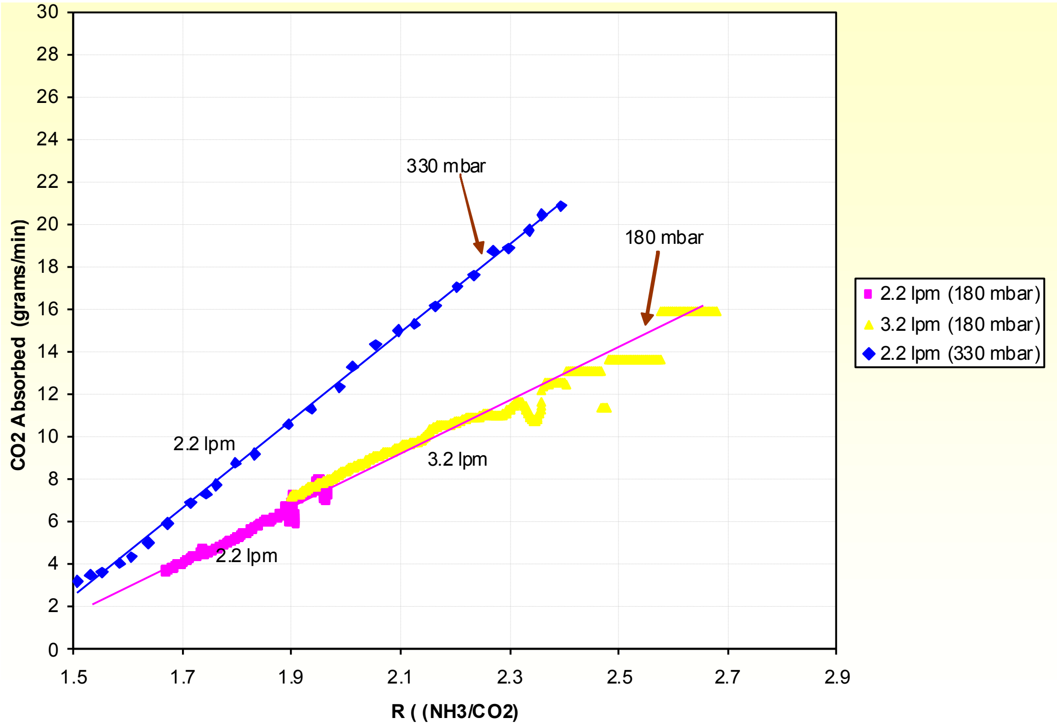

Figure 9: The effect of liquid recirculation rate at 22° C and 180 mbar.

Stripper Analysis

Experiments were performed to investigate the variation of ammonia removal with reboiler temperature for 2.8 M ammonia feed solution with a feed rate of 0.4 lpm. Additional results are shown for the percentage ammonia removal during testing with a 1,000 ppm ammonia solution at a feed rate of 1 lpm. These results are shown in Figure 10. Data from these experiments indicates that the residual NH_3 level in the bleed water is a strong function of the temperature of the reboiler. For example, decreasing the temperature from 56° to 54°C, increases the residual NH_3 level from 500 to 3000 ppm under these test conditions. The pressure inside the column was nearly same as the vapor pressure of water at the bottoms of the column indicating the pressure drop across the column was negligibly small.

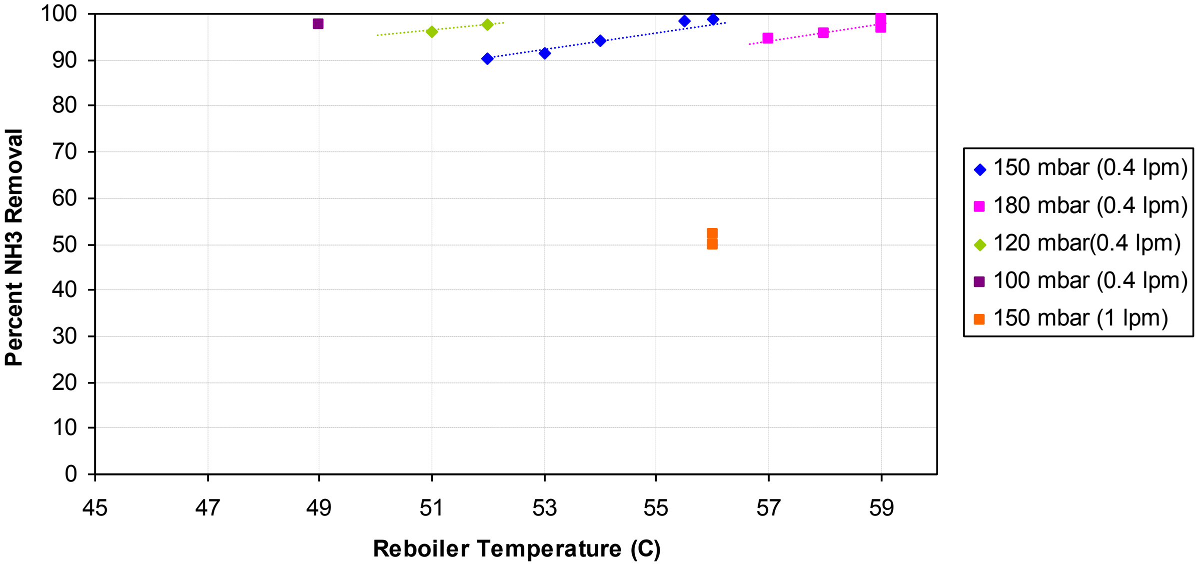

Figure 10: Percent removal of NH_3 calculated by measurements of NH_3 in the bleed solution as a function of temperature, pressure, and feed flow rate.

Repeated cycles of distillation with dilute draw solutions at 1 l/min and 100 mbar were performed to achieve ultra-trace levels of NH_3 in the product water. This data is shown in Figure 11. The stripper bottoms temperature was between 45 and 50 °C during operation and increased with decreasing concentration of NH_3 in the stripper bottoms. The initial solution containing ~930 ppm of NH_3 was distilled in the stripper producing a solution that contained ~400 ppm of NH_3. The process was repeated nine (9) times to achieve a water that contained ~2 ppm NH_3. Equilibrium modeling using process simulation software shows that a single column pass was equivalent in removal performance to a single theoretical stage. The chosen packing provided a relatively low pressure drop under the liquid flow rate used in bench-scale stripper experiments. The dilute draw solution flow rate of 1 lpm corresponds to a liquid velocity of 3 gal/min-ft^2. The estimated steam flow rate is about 3.6 g/s and the manufacturer reported F_s factor is ~1.1 ft/s*(lb/ft^3)^0.5. These values provide a pressure drop of 0.11-in H_2O/ft of packing and with 16 ft of packing, the pressure drop will be 1.8-in water gauge or 4.4 millibar. Increasing the liquid flow rate to 2 l/min (Liquid velocity = 6.0 gpm/$ft^2$and F_s = 2.3 ft/s*(lb/ft^3)^0.5) will lead to a pressure drop of 0.8 in H_2O/ft (2 mbar/ft). At a packing height of 16 ft this pressure drop is a significant value in an operation where the reboiler temperature is 50°C and the vapor pressure of water is 100 mbar.

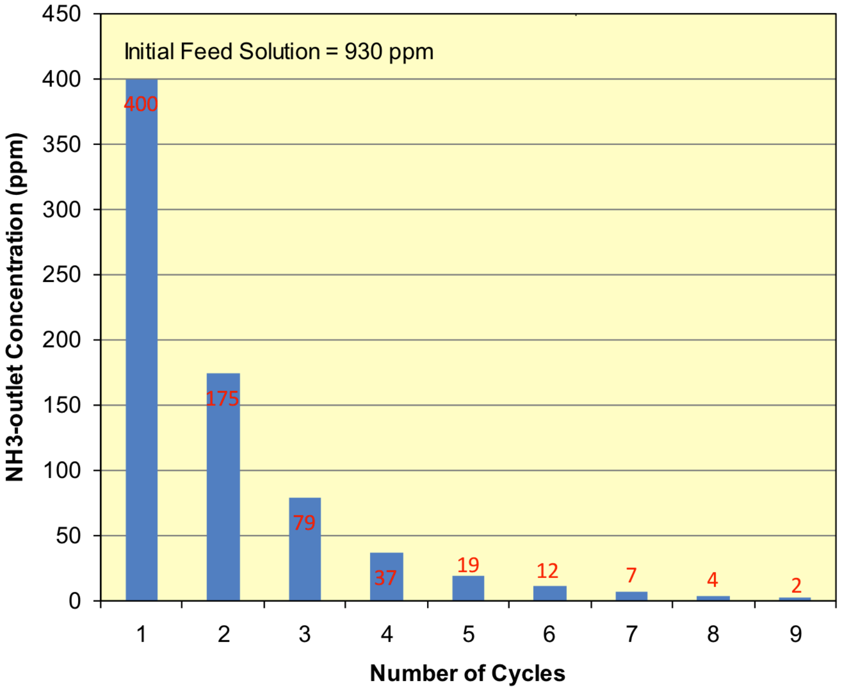

Figure 11: Residual level of ammonia in the stripper bottoms water as a function of the number of throughput cycles (corrected for small changes in the feed concentration at various stages).

The structural packing used in the bench-scale stripper removed a substantial fraction of the NH_3 from the solution; yet the performance measurements recorded may not be optimum because of liquid wall channeling. This wall effect is more prominent in small diameter strippers than in large diameter, commercial strippers.

Task 3: Stripper Subsystem Development

Additional stripping analysis was performed at atmospheric pressure with a focus on achieving < 1 mg/L of NH_3 in the stripper bottoms while recovering all of the overhead vapors with a condenser and without the need for an additional absorber. During this series of testing the composition of the draw solution was approximately 84.4% H_2O, 6.8% NH_3, and 8.8% CO_2 on a mass fraction basis. For each test the stripper reboiler duty was estimated using the process mass balance and temperature data collected. Vapor rate leaving the stripper as a function of the calculated reboiler duty is shown in Figure 12. There is a positive correlation between the amount of power input to the reboiler and mass flow of vapor out of the column; however, it is important to note that the speciation of the vapor changes substantially as the bottoms receive more heat. The higher vapor pressure of NH_3 and CO_2 mean that these two gases will vaporize to a greater extent than water vapor at a given temperature. After majority of the NH_3 and CO_2 is driven from the solution an increasing mass fraction of water is evaporated. The energy penalty for overcoming the enthalpy of vaporization for water versus that required for thermal decomposition of CO2NH2- and the vaporization of NH_3 and CO_2 must be minimized during design of commercial Oasys systems. Practically, the amount of power input to the reboiler is controlled by the product water specification for residual NH_3 and will vary for different applications of the technology.

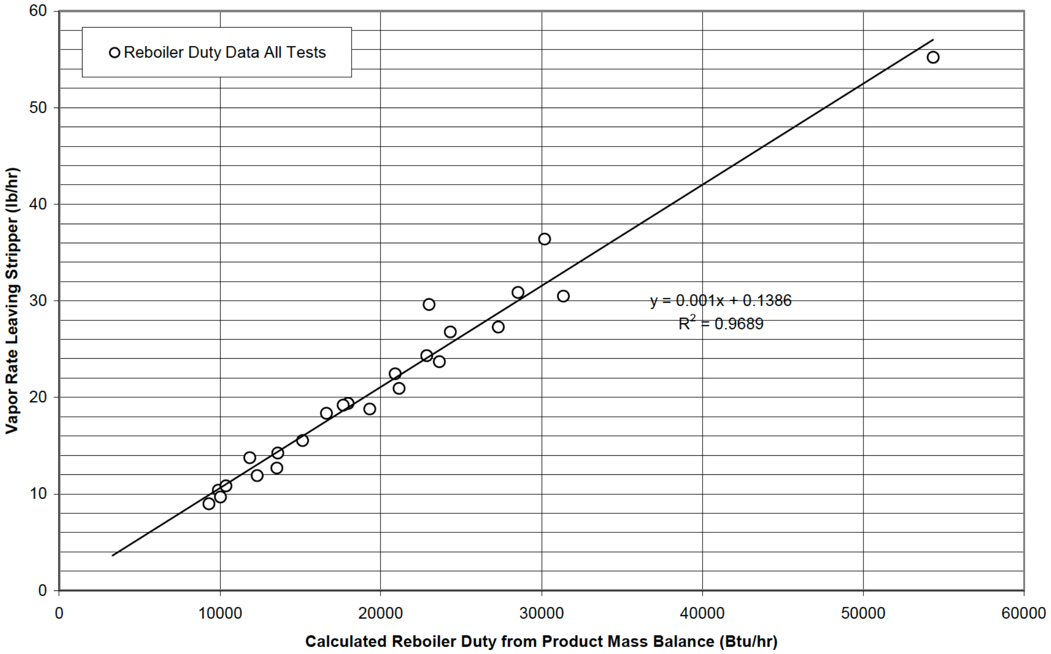

Figure 12: Vapor rate as a function of reboiler duty for tests conducted at atmospheric pressure.

Additional atmospheric pressure stripper experimental work was performed to obtain optimum operating conditions of the stripper, determine the HETP of the packing under stripping conditions and to develop design parameters for commercial systems. Table 1 provides a summary of different experimental runs performed under slightly varying conditions. For the application being evaluated, achieving NH_3 concentration in the product water (or sump of the stripper) of less 10 mg/L is acceptable and was demonstrated through this testing. Later, this data will be compiled with improved process simulation models to determine the HETP for the packing employed in this testing.

Table 1: Summary of testing conditions during various runs with advanced pilot scale stripper column. Concentrated draw solution (CDS) produced by stripping the NH_3 and CO_2 from the solution and fully condensing the vapor.

Parameter	Unit	Test 1	Test 2	Test 3	Test 4
Sump temperature	K	377.70	377.43	377.17	377.17
Column inlet feed temperature (discharge of preheater)	K	362.19	361.73	361.82	362.72
Reboiler inlet temperature	K	375.97	375.79	375.51	375.38
Reboiler discharge temperature	K	377.50	377.23	376.96	376.98
Temperature of vapor leaving the top of stripper	K	361.67	361.38	361.06	362.24
Sump Pressure	atm	1.15	1.14	1.13	1.14
Reboiler discharge pressure	atm	1.16	1.15	1.14	1.14
Pressure of vapor leaving the top of stripper	atm	1.11	1.10	1.09	1.09
DDS inlet flow rate	kg/hr	98.88	99.25	101.97	89.81
Product water flow rate	kg/hr	73.57	74.84	75.84	67.04
CDS "N" conc	M	11.39	14.79	15.54	16.52
CDS "C" conc	M	4.34	5.97	6.16	6.71
Ammonia conc in sump	ppm	3.10	<1	2.35	3.40

Task 4: Absorption Subsystem Development

A critical parameter that affects the overall ability of the vaporized draw solution solutes to condense and absorb back into an aqueous draw solution is the absorption kinetics of CO_2. To improve the solubility of NH_3/CO_2 draw solutions it is necessary to favor N:C molar ratio in excess of unity [22]. During the absorption of NH_3 and CO_2 back into a highly concentrated draw solution NH_3 tends to rapidly overcome the gas film and partition into the aqueous phase and is not the rate-limiting step. CO_2, on the other hand, must partition into a weak alkaline solution where it acts as a diprotic acid, speciates according to solution pH, and reacts with aqueous ammonia to form $CO_2NH_2^-$ in an exothermic reaction. Within this context, the liquid film resistance for CO_2 is much greater compared to its gas film resistance and also requires a rate limiting reaction in the formation of $CO_2NH_2^-$. To improve our understanding of the kinetics of CO_2 absorption, and to confirm thermophysical models that predicts the extent of $CO_2NH_2^-$ formation we conducted a series of absorption experiments with a well-insulated knockout pot. The knockout pot (reactor) was charged with a 4 M NH_4OH solution and CO_2 gas was bubbled into the reactor at a constant flow rate while the temperature of the solution was monitored as shown in Figure 6.

A plot of the reactor tops temperature as a function of time for a representative experiment is shown in Figure 13. Carbamate formation increases as more CO_2 is exposed to the aqueous ammonia solution. Eventually the solution reaches saturation with respect to CO_2 and all available NH_3 is converted into $CO_2NH_2^-$. At this point the solution ceases to generate heat from the exothermic reaction and the system reaches steady state. Assuming the specific heat capacity of CO_2 gas at 298.15 K is 0.202 cal/g-C and the 4 M aqueous NH_3 solution may be approximated as water with a heat capacity of 1.0 cal/g-C [34], a mass and energy balance of the adiabatic system yields the carbamate formation as shown in Table 2.

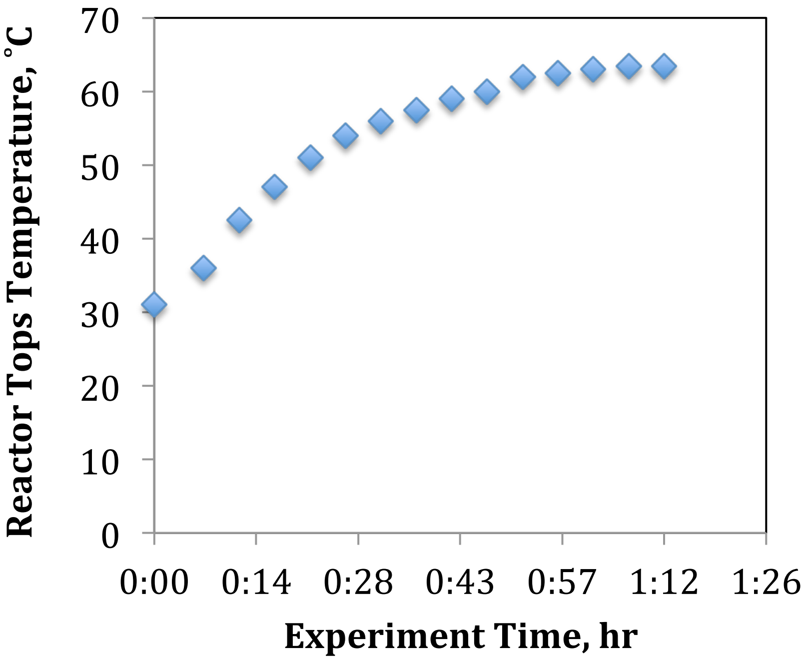

Figure 13: Reactor tops temperature as a function of time for a representative absorption experiment.

Table 2: Experiment parameters and associated mass and energy balance to determine the extent of $CO_2NH_2^-$ conversion.

Parameters	Value	Unit
Initial Solution Mass	21.0	lb
CO_2 Injected	3.5	lb
Temperature Increase	27.5	˚C
Heat Absorbed	261,957	cal
Heat Consumed by CO_2 Injection	12,511	cal
Max Potential Heat Evolution (Assuming Full Conv.)	621,661	cal
Heat Available	609,150	cal
Percent conversion to $CO_2NH_2^-$	43	%

Task 5: Modeling the Absorption and Stripper Columns Performance

Absorber Data Integration

The operation of the absorber was modeled using Aspen Plus. The simulation model has been validated and refined using experimental measurements. The simulation model is then used for augmenting experimental measurements by performing what-if scenario. The simulation model has been updated to perform absorber (condenser) designs operating under commercial operating conditions.

The data provided by the knockout pot study is in good agreement with process simulation models. During design of systems the heat evolution associated with the formation of $CO_2NH_2^-$ must be accounted for and removed from the system to enable continued formation of $CO_2NH_2^-$ without incurring counterproductive decomposition of the thermolytic solutes at elevated absorber temperatures. It is also important to note that the reaction kinetics of CO_2 gas absorption and subsequent reaction to form $CO_2NH_2^-$ may be improved through inducing turbulence in the liquid phase and increasing contact time of the gas-liquid exchange, thus improving CO_2 conversion from the liquid film into the bulk liquid phase. Process models also confirm that the kinetics of the formation reaction for $(NH_4)_2CO_2$ is substantially slower than the formation of $NH_4CO_2NH_2$.

Solution Properties Modification to Improve Process Simulation Software Accuracy

Aspen PLUS thermophysical property databases were improved to more accurately reflect the empirically derived properties of known NH_3/CO_2 solutions. In particular, improvements in properties such as solution density, partial vapor pressures of NH_3, CO_2, and H_2O, and total solution pressure as a function of solution composition and temperature were made and substantially increase the reliability of process simulations with the software. Parity plots from our empirical data sets and process simulation models for total pressure, CO_2 partial pressure, and solution density is shown in Figure 14 through Figure 16. The data sets demonstrate the substantial improvement in the ability of the process simulation models to accurately calculate these parameters and can be seen by the proximity of data points to the parity line (slope = 1) where the calculated and measured properties are in perfect agreement.

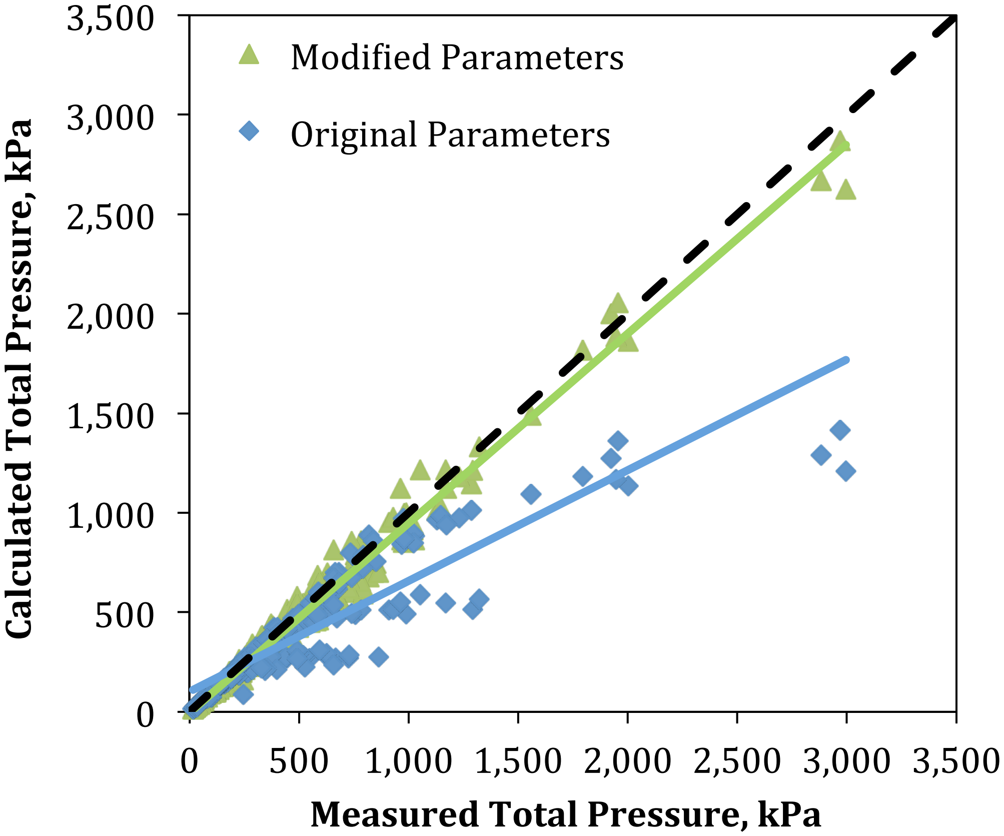

Figure 14: Parity plot of the measured and process simulation calculated total pressure for a variety of NH_3/CO_2 mixtures.

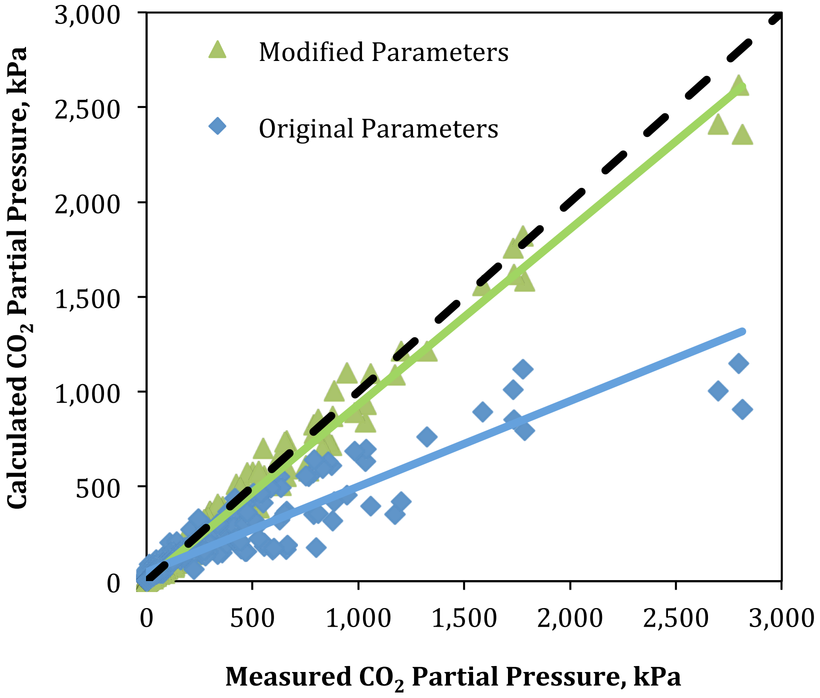

Figure 15: Parity plot of the measured and process simulation calculated partial pressure of CO_2 for a variety of NH_3/CO_2 mixtures.

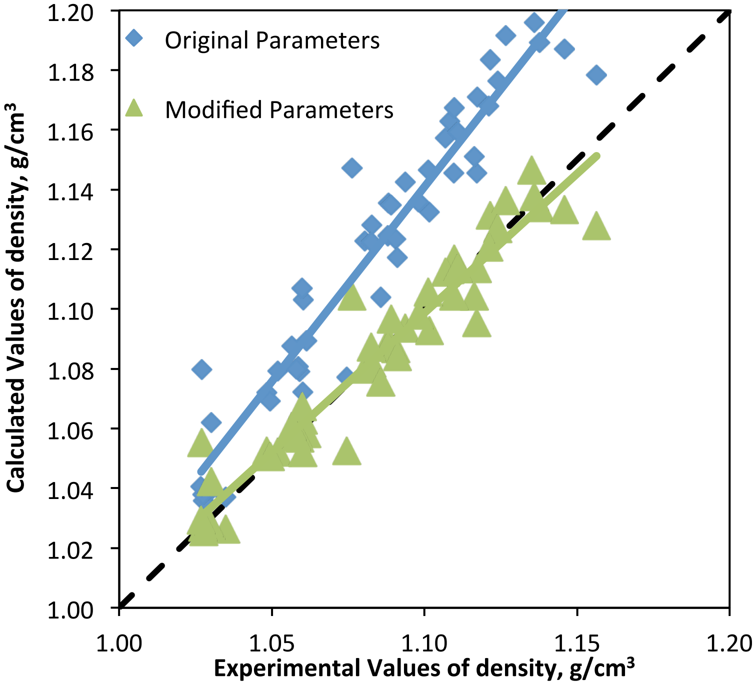

Figure 16: Parity plot of the measured and process simulation calculated solution density for a variety of NH_3/CO_2 aqueous mixtures.

The operation of the stripper was modeled using Aspen Plus. The simulation model was validated and refined using experimental measurements. The simulation model is then used for augmenting experimental measurements by performing what-if scenarios. Much of this data is confidential in nature and cannot be disclosed in this document. The simulation model was updated to evaluate stripper designs operating under commercial operating conditions. As an example, data from the second test shown in Table 1 was modeled with Aspen PLUS and the results and HETP analysis are summarized in Table 3. This data is representative of column performance prior to optimization steps such as achieving optimal liquid loading, reboiler duty, preheat temperature, operating pressure, or packing configuration. The HETP and column height for this simulation is sufficient for the stripping of DDS to less than 1 mg/L NH_3 in the product water and generation of fully condensed concentrated draw solution (CDS) suitable for the treatment of high salinity brines exceeding 200,000 mg/L TDS.

Table 3: Comparison of stripper process experimental run with simulated process results and subsequent key process performance parameters.

Parameter	Unit	Test 2	Simulated
Sump temperature	K	377.43	377.17
Column inlet feed temperature (discharge of preheater)	K	361.73	362.72
Reboiler inlet temperature	K	375.79	375.38
Reboiler discharge temperature	K	377.23	376.98
Temperature of vapor leaving the top of stripper	K	361.38	362.24
Sump Pressure	atm	1.14	1.14
Reboiler discharge pressure	atm	1.15	1.14
Pressure of vapor leaving the top of stripper	atm	1.10	1.09
DDS inlet flow rate	kg/hr	99.25	89.81
Product water flow rate	kg/hr	74.84	67.04
CDS "N" concentration	M	14.79	16.52
CDS "C" concentration	M	5.97	6.71
Ammonia concentration in sump	ppm	<1	3.40
Calculated steam input	kW		12.20
Estimated steam input from table	kW		17.09
Calculated steam input efficiency	%		71.39
Number of separation stages			16
HETP	ft		1.88

Accomplishments

During this study numerous improvements were made to the process knowledge and understanding associated with the thermal management of aqueous solutions with NH_3 and CO_2 derived electrolytes employed for water treatment using EO technology. Stripping of simulated synthetic draw solution solutes and the subsequent condensation and absorption of the vapor to regenerate the draw solution for reuse within an Oasys EO system was demonstrated under numerous operating conditions. Product water (stripper bottoms) with NH_3 concentration less than 1 mg/L was demonstrated. Full condensation and recapture of all vaporized draw solution solutes were achieved with several bench-, pilot-, and demonstration-scale stripper installations. Lastly, empirical data from the literature as well as experiments conducted at Oasys Water were successfully assimilated into process simulation software to improve the accuracy of EO system engineering design compared to the best existing product on the market.

Oasys Water is actively pursuing commercial application of this technology in a variety of water purification and waste management markets, in addition to renewable energy generation through our proprietary osmotic heat engine. More information on our recent success in piloting a fully integrated, demonstration-scale Oasys membrane brine concentrator (MBC) process with EO technology for fracture flowback and produced water brine treatment may be found in our recent publication in the journal Desalination [24]. More information on the company may be found at www.oasyswater.com, which also serves to catalog company disclosures in both scientific and trade journals. Work related to the research contained in the body of this report was presented at numerous professional and industry conferences including major meetings of the American Water Works Association (AWWA), the American Institute of Chemical Engineers (AIChE), the American Membrane Technology Association (AMTA), and the International Desalination Association (IDA).

Conclusions

Near complete thermal stripping of NH_3 and CO_2 from an aqueous solution cannot be done selectively with respect to water vapor. To achieve very low NH_3 concentrations in the stripper sump, it is necessary to heat the fluid to a temperature near the boiling point of the solvent at the pressure of operation, whereby additional heat is being consumed in the vaporization of water. A rectifier section could be added to the tops of the stripper column to further improve the purity of the vapor stream with respect to pure NH_3 and CO_2; however, the presence of water vapor is helpful in the subsequent condensation and absorption step. The benefit of reducing the bottoms concentration of ammonia, thus reducing thermal energy input for a given system, must be considered with respect to application requirements, but will reduce power demand for the system. If a loss of NH_3 in the product water is acceptable for a given application, additional analysis may also be required to determine the cost of replacement for draw solution solutes bled from the draw solution loop.

Thermal management in absorber systems is critical to facilitate the absorption of CO_2 and subsequent formation of $NH_2CO_2^-$ in an NH_4^+ rich environment. Operating with N:C molar ratios exceeding 2:1 can substantially improve the absorption rate of CO_2 in such systems, but this operating condition must also consider the impact on the membrane subsystem. In commercial systems that employ thermal sources with temperatures in excess of 100 ˚C it is possible to perform complete condensation of the overhead vapor without the need for an additional absorption column. Systems that employ low-grade thermal sources may require an absorption unit process, but this may be avoided with improvements to overall process design and operating conditions enforced on the tops vapor.

Recommendations

Most future research and development activities are not available for public disclosure, but generally focus on methods to improve the thermal efficiency of the draw solution stripping method and optimize vapor condensation and absorption. Stripping columns are very mature, robust technologies; however, additional research and development efforts aimed at improving column packing materials and optimizing liquid loading rates in the column may have substantial positive impact on system design. Additional development effort is directed to the development of alternative methods to strip and absorb thermolytic solutes. Some near term technologies that may be employed for this process include membrane contactors that can be operated in direct contact, air gap, or vacuum modes to impart a vapor pressure gradient across a hydrophobic microporous membrane and strip solutes with partial vapor pressures lower than water. These systems have also been investigated as gas absorbers for a number of diverse applications [35] and may serve a similar function for the absorption of thermolytic solutes in EO systems. The biggest hurdle for this application is the thermal management of the warming concentrated draw solution during the exothermic $NH_2CO_2^-$ formation reaction.

Commercialization of this technology is focused on several vectors to market. In some applications the use of high-grade thermal sources is preferred; however, for large markets, like the integration of renewable thermal sources for large scale municipal desalination, additional work is required to optimize EO system integration and thermal management. Additionally, EO technology may be employed to harvest electrical power from low-grade thermal sources. System development for this application is underway and early results for integration with bottom cycling systems in enhanced geothermal systems are promising.

References

[1] S. Zhao, L. Zou, C.Y. Tang, D. Mulcahy, Recent developments in forward osmosis: Opportunities and challenges, J. Membr. Sci., 396 (2012) 1-21.

[2] A. Achilli, A.E. Childress, Pressure retarded osmosis: From the vision of Sidney Loeb to the first prototype installation -- Review, Desalination, 261 (2010) 205-211.

[3] L.A. Hoover, W.A. Phillip, A. Tiraferri, N.Y. Yip, M. Elimelech, Forward with Osmosis: Emerging Applications for Greater Sustainability, Environ. Sci. Technol., 45 (2011) 9824-9830.

[4] T.Y. Cath, A.E. Childress, M. Elimelech, Forward osmosis: principles, applications, and recent developments, J. Membr. Sci., 281 (2006) 70-87.

[5] E.G. Beaudry, K.A. Lampi, Membrane technology for direct osmosis concentration of fruit juices, Food Technology, 44 (1990) 121.

[6] R.J. York, R.S. Thiel, E.G. Beaudry, Full-scale experience of direct osmosis concentration applied to leachate management, in: Proceedings of the Sardinia '99 Seventh International Waste Management and Landfill Symposium, S. Margherita di Pula, Cagliari, Sardinia, Italy, 1999.

[7] D.K. Anderson, Concentration of dilute industrial waste by direct osmosis, in: chemical engineering, University of Rhode Island, Providence, 1977, pp. 182.

[8] T.Y. Cath, N.T. Hancock, C.D. Lundin, C. Hoppe-Jones, J.E. Drewes, A multi-barrier osmotic dilution process for simultaneous desalination and purification of impaired water, J. Membr. Sci., 362 (2010) 417-426.

[9] N.T. Hancock, N.D. Black, T.Y. Cath, A comparative life cycle assessment of hybrid osmotic dilution desalination and established seawater desalination and wastewater reclamation processes, Water Res., 46 (2012) 1145-1154.

[10] K.L. Hickenbottom, N.T. Hancock, N.R. Hutchings, E.W. Appleton, E.G. Beaudry, P. Xu, T.Y. Cath, Forward osmosis treatment of drilling mud and fracturing wastewater from oil and gas operations, Desalination, (2012), doi: (10.1016/j.desal.2012.05.037).

[11] J.L. Cartinella, T.Y. Cath, M.T. Flynn, G.C. Miller, K.W. Hunter, A.E. Childress, Removal of natural steroid hormones from wastewater using membrane contactor processes, Environ. Sci. Technol., 40 (2006) 7381-7386.

[12] T.Y. Cath, V.D. Adams, A.E. Childress, Membrane contactor processes for wastewater reclamation in space. II. Combined direct osmosis, osmotic distillation, and membrane distillation for treatment of metabolic wastewater, J. Membr. Sci., 257 (2005) 111-119.

[13] R.L. McGinnis, M. Elimelech, Global Challenges in Energy and Water Supply: The Promise of Engineered Osmosis, Environ. Sci. Technol., 42 (2008) 8625-8629.

[14] B. Mi, M. Elimelech, Chemical and physical aspects of organic fouling of forward osmosis membranes, J. Membr. Sci., 320 (2008) 292-302.

[15] B. Mi, M. Elimelech, Organic fouling of forward osmosis membranes: Fouling reversibility and cleaning without chemical reagents, J. Membr. Sci., 348 (2010) 337-345.

[16] S. Lee, C. Boo, M. Elimelech, S. Hong, Comparison of fouling behavior in forward osmosis (FO) and reverse osmosis (RO), J. Membr. Sci., 365 (2010) 34-39.

[17] W.C.L. Lay, T.H. Chong, C.Y.Y. Tang, A.G. Fane, J.S. Zhang, Y. Liu, Fouling propensity of forward osmosis: Investigation of the slower flux decline phenomenon, Water Science Technology, 61 (2010) 927-936.

[18] N.T. Hancock, P. Xu, D.M. Heil, C. Bellona, T.Y. Cath, Comprehensive Bench- and Pilot-Scale Investigation of Trace Organic Compounds Rejection by Forward Osmosis, Environ. Sci. Technol., 45 (2011) 8483-8490.

[19] M. Xie, L.D. Nghiem, W.E. Price, M. Elimelech, Comparison of the removal of hydrophobic trace organic contaminants by forward osmosis and reverse osmosis, Water Res., 46 (2012) 2683-2692.

[20] D.L. Shaffer, N.Y. Yip, J. Gilron, M. Elimelech, Seawater desalination for agriculture by integrated forward and reverse osmosis: Improved product water quality for potentially less energy, J. Membr. Sci., 415–416 (2012) 1-8.

[21] R. Semiat, Energy Issues in Desalination Processes, Environ. Sci. Technol., 42 (2008) 8193-8201.

[22] R.L. McGinnis Osmotic desalination process. US200202740, 2002.

[23] J.R. McCutcheon, R.L. McGinnis, M. Elimelech, A novel ammonia-carbon dioxide forward (direct) osmosis desalination process, Desalination, 174 (2005) 1-11.

[24] R.L. McGinnis, N.T. Hancock, M. Nowosielski-Slepworan, G.D. McGurgan, Pilot demonstration of the NH3/CO2 forward osmosis desalination process on high salinity brines, Desalination, in press (2013).

[25] J.C. Crittenden, R.R. Trussell, D.W. Hand, K.J. Howe, G. Tchobanoglous, Water Treatment: Principles and Design, 2 ed., Wiley, New Jersey, 2005.

[26] M. Wilf, The Guidebook to Membrane Desalination Technology, Balaban Deslination Publications, L'Aquila, 2007.

[27] M. Elimelech, W.A. Phillip, The Future of Seawater Desalination: Energy, Technology, and the Environment, Science, 333 (2011) 712-717.

[28] M. Mulder, Basic principles of membrane technology, 2nd ed. ed., Kluwer Academic Publishers, Dordrecht, The Netherlands, 1997.

[29] IDA Worldwide Desalting Plants Inventory; 19; Global Water Intellegence: Gnarrenburg, Germany, 2006.

[30] U. Göppert, G. Maurer, Vapor—liquid equilibria in aqueous solutions of ammonia and carbon dioxide at temperatures between 333 and 393 K and pressures up to 7 MPa, Fluid Phase Equilib., 41 (1988) 153-185.

[31] F. Kurz, B. Rumpf, G. Maurer, Vapor-liquid-solid equilibria in the system NH3 □ CO2 □ H2O from around 310 to 470 K: New experimental data and modeling, Fluid Phase Equilib., 104 (1995) 261-275.

[32] A. Ghaemi, S. Shahhosseini, M.G. Maragheh, Nonequilibrium dynamic modeling of carbon dioxide absorption by partially carbonated ammonia solutions, Chem. Eng. J., 149 (2009) 110-117.

[33] Produced Water Market: Opportunities in the Oil, Shale, and Gas Sectors in North America; Global Water Intelligence: Oxford, 2011.

[34] R.H. Perry, D.W. Green, Perry's Chemical Engineers' Handbook (7th Edition), in, McGraw-Hill, 1997.

[35] B.W. Reed, M.J. Semmens, E.L. Cussler, Membrane contactors, Membrane Separation Technology, (1995) 474.